

Off-axis Fiber Bragg Grating Fabricated by Femtosecond Laser Direct Writing for Torsion Sensing

Duarte Viveiros^{1,2,*}, José M. M. de Almeida^{1,3}, L. Coelho¹, João M. Maia^{1,2}, Vítor A. Amorim^{1,2}, Pedro A. S. Jorge^{1,2} and P. V. S. Marques^{1,2}

¹Center for Applied Photonics, INESC TEC, Rua Dr. Roberto Frias, 4200-465 Porto, Portugal;

²Department of Physics and Astronomy, Science Faculty, University of Porto, Rua do Campo Alegre, 4169-007 Porto, Portugal;

³Department of Physics, School of Science and Technology, University of Trás-os-Montes and Alto Douro, Quinta de Prados, 5001-801 Vila Real, Portugal.

*carlos.d.viveiros@inesctec.pt

Abstract: The precise production of 4.5 μm off-axis first order FBG in an SMF-28e fiber through femtosecond laser direct writing is demonstrated. The off-axis FBG potential as sensing head for torsion sensing was successfully explored.

OCIS codes: (260.1440) Birefringence; (060.3735) Fiber Bragg gratings; (060.2370) Fiber optics sensors; (060.2430) Fibers, single-mode; (320.7090) Ultrafast lasers.

1. Introduction

Fiber Bragg Gratings (FBGs) are one of the most important passive optical components in the fields of optical communications and sensor systems [1, 2]. Their most important features include the simplicity of operation, the flexibility they offer for achieving specific spectral characteristics, the fabrication in different types of optical fibers, absolute encoding, and batch fabrication [1, 2]. Traditionally, fiber gratings are conventionally inscribed into the core of photosensitive single-mode fibers (SMF) using ultraviolet (UV) laser exposure through phase mask or holographic methods [3, 4]. The femtosecond (fs) laser direct writing technique used in this work opens the possibility to inscribe gratings not only inside the core volume but also in the fiber cladding surrounding the core with high spatial resolution due to the underlying non-linear light-matter interaction [5]. With the present technique, there is no need for a phase mask or hydrogen loading, and it has excellent design flexibility, enabling a high level of customization of grating parameters, such as length, bandwidth, or Bragg wavelength [5, 6]. Using the Bragg relation, it is possible to calculate the Bragg wavelength, which is given by $\lambda_B = 2 \times n_{eff} \times (v/f_{mod})$, where v is the velocity of the stage and, n_{eff} the effective index of refraction of the guided mode. In turn, the Bragg wavelength can easily be controlled by simply tuning the modulation frequency, f_{mod} [5].

The most common physical parameters measured using FBGs sensors are temperature, strain, curvature, or pressure, either individual or simultaneously, through wavelength monitoring or power detection [2]. Recently, torsion measurements have been the subject of research [7]. Optical torsion sensors involving high- or low-birefringence photonic crystal fibers in Sagnac loops, high-birefringence (Hi-Bi) fiber demodulated using a Hi-Bi FBG, corrugated long-period fiber gratings, integrated single-mode fibers, multicore fibers, polarization-maintaining fibers, fiber ring laser, inscriptions of FBGs, and some special fibers are examples of the work developed for torsion measurement [7 – 9]. However, some of these sensors present complex fabrication processes which render difficult its implementation in practical applications [8, 10].

In this work, the fabrication of first order off-axis FBG in an SMF through fs-laser direct writing is demonstrated and implemented on a torsion setup. The polarization properties for torsion measurement are demonstrated through the reflected intensity ratio, which enables the simultaneous measurement of the torsion and discriminates the torsion direction. The relatively low complexity and the robust nature of the fabricated device open the possibility to be used in practical applications, such as structural health monitoring.

2. Fabrication and Characterization Setups

A femtosecond (fs) laser direct writing system was developed to explore the fabrication of FBGs inside a standard single-mode fiber (SMF-28e, Corning) through a localized refractive index (RI) modifications. The writing system is composed of a fiber amplified fs-laser (Satsuma HP, from Amplitude Systèmes), providing a second harmonic beam at 515 nm, with a pulse duration of ~ 250 fs at a repetition rate of 500 kHz. The laser beam was focused on the core-cladding boundary with a $100\times$ oil immersion lens (Olympus PLN 100XO), 1.25 numerical aperture, which is mounted on a Y (Newport MILS150CC) and Z (Newport VP-25XA) precision linear stages. For the writing process, it's necessary to remove the optical fiber coating around the writing section and carefully clean that using ethanol.

Then, the bare fiber is clamped to two three-axis positioners (MBT616/M, Thorlabs) that are mounted on the X air-bearing linear stage (ABL10100-LN). It is also required kept the optical fiber under tension (1 N) to remove the curvature during the writing process and to ensure that it remains in position. An index matching liquid (Cargille cat#19571, RI = 1.4587) to eliminate the cylindrical aberration, due to the fiber geometry, and to compensate for the RI mismatch at the surface of the optical fiber is used. So, the optical fiber is immersed in the liquid and imaged through the writing objective onto a CCD camera, allowing a precise positioning of the Bragg grating. During writing, the laser gate was externally controlled by a periodic square function with a duty cycle of 50 % generated by a synthesized function generator (DS345, Stanford Research Systems) [11]. This simple arrangement allows the automated writing of gratings by simply translating the optical fiber at constant velocity along X, with the signal modulation turned on. More details regarding the alignment and writing processes were previously published by the authors [11]. The grating period and length were defined to be 535.44 nm and 15 mm, respectively. The optimal writing conditions for the off-axis FBG was found to be 140 nJ of pulse energy, 50 $\mu\text{m/s}$ of scanning velocity, fiber tension of 1 N, and a writing beam polarization aligned with the scanning direction of the fiber.

The spectral features of the off-axis FBG during the fabrication process was monitored with a customized setup composed by a broadband light source (model ASE2000), ranging from 1525 to 1610 nm, an optical circulator and an optical spectrum analyzer (OSA, model Yokogawa AQ6370D) with a resolution of 0.02 nm to acquire the transmitted and the reflected spectra. All spectra were measured without polarization control and normalized to the transmitted spectrum of the light source.

The polarization dependence of the off-axis FBG was evaluated, inserting a polarizer before the grating structure in the characterization setup. Therefore, the signal reflected in the FBG without torsion was measured with polarization control. Adjusting the polarizer orientation, it was possible to get one of the two polarization modes separately for the fast (Y) and slow (X) axes.

For torsion measurements, the 4.5 μm off-axis FBG was positioned in the middle of the set-up, and the ends of the fiber were clamped by two fiber holders separated by 4 cm. One end of the fiber was fixed to a static holder, while the other end was fixed to a controllable rotary holder which rotates clockwise or anticlockwise along the cross-section of the fiber, as shown in Fig. 1. The rotary holder was rotated up to 6.28 rad in steps of 0.52 rad, so the maximum torsion step applied to the off-axis FBG was 157.08 rad/m.

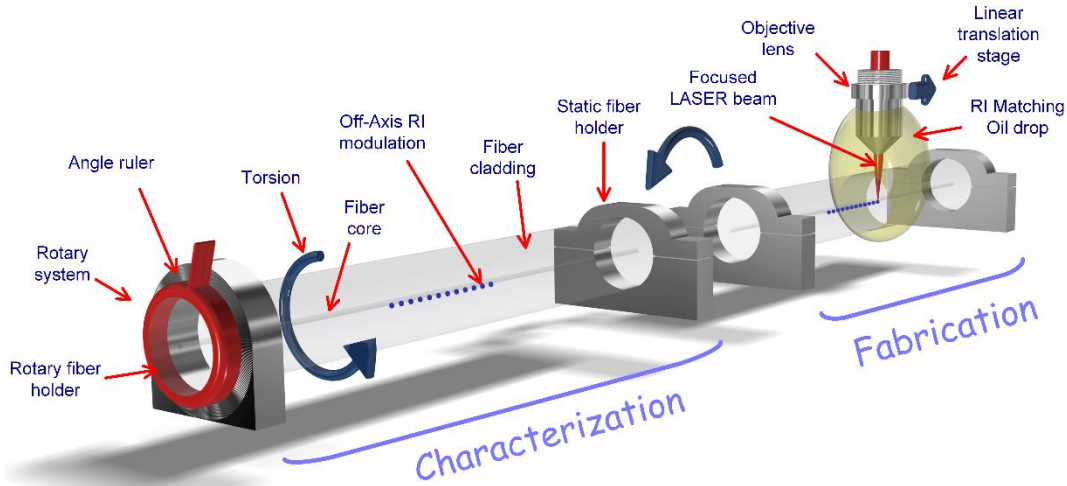


Fig. 1. Schematic illustration of the fabrication and Characterization processes of 4.5 μm off-axis FBG.

3. Experimental results and discussion

The off-axis FBG with 4.5 μm offset from the core center is accomplished by the grating inscription over the core-cladding boundary, as shown in Fig. 2 (a). This inscription is possible due to the high precision optical fiber position system. The transmitted and reflected spectra of the off-axis FBG under fabrication tension (1 N) are presented in Fig. 2 (b).

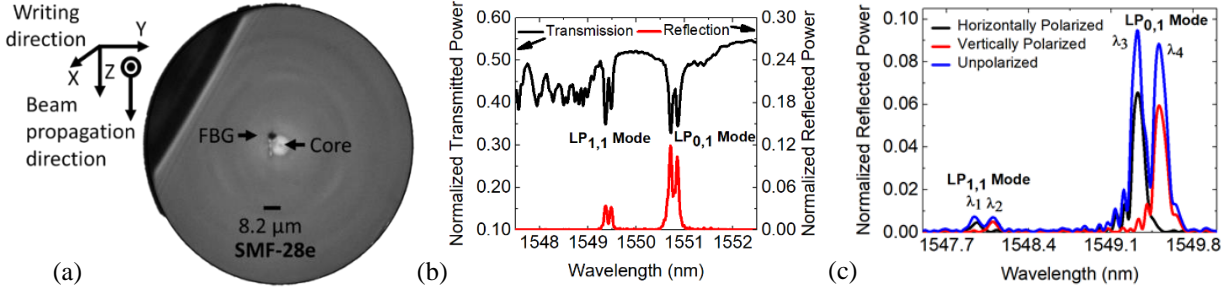


Fig. 2. Off-axis FBG with 4.5 μm offset from the core center: (a) end-view optical micrograph, (b) transmission and reflection spectra, and (c) unpolarized, vertical and horizontal linearly polarized optical reflection spectra.

The end view section image presented in Fig. 2 (a) shows the increase of the effective core size in the section where the FBG is inscribed. The resulting transmission spectra consist of a strong Bragg resonance with two peaks, due to birefringence induced by the asymmetric structure, and several cladding mode resonances on the short wavelength side. The existence of an additional Bragg resonance is visible in the reflection spectra and explained with the increase of the core size and its RI, which increases the V-number. When the V-number is lower than 2.405, only one linearly polarized mode ($LP_{0,1}$) can propagate along the single-mode optical fibers at the wavelength λ . This increase of the V-number above the cutoff condition means that the fiber section where the off-axis FBG is written turns into a multimode section that supports the modes $LP_{0,1}$ and $LP_{1,1}$ [12]. The reflection spectra without torsion were measured by adjusting the polarizer orientation to get one of the two polarization modes separately, as shown in Fig. 2 (c). The different Bragg resonance peak associated with each polarization axis was used to determine the degree of birefringence through the equation, $\Delta n_B = (\lambda_{B2} - \lambda_{B1})/2\Lambda$ [13]. Therefore, for the two Bragg resonances of each mode ($LP_{1,1}$ and $LP_{0,1}$) separated by 139 and 181 pm, the birefringence of 1.3×10^{-4} and 1.7×10^{-4} , respectively, was estimated.

The fiber torsion process results in a perturbation of the RI profile nonuniformly over its cross-section, so the characterization of the off-axis FBG to torsion was performed, and the results presented in Fig. 3.

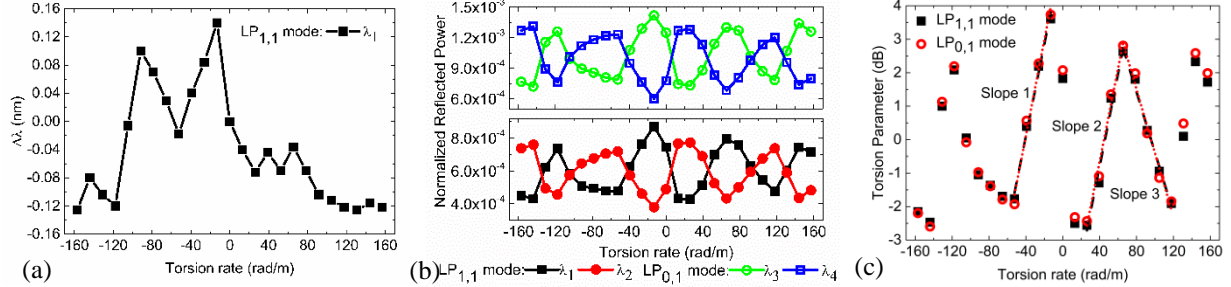


Fig. 3. Spectral analysis of the off-axis FBG: (a) wavelength shift, (b) normalized reflected power, and (c) torsion parameter as a function of the torsion rate.

As shown in Fig. 3, when the fiber is subjected to torsion, the wavelength and the intensity response of both Bragg wavelengths of the $LP_{1,1}$ and $LP_{0,1}$ modes changed as the torsion rate was applied. In Fig. 3 (a) and (b) the lines connecting symbols are a guide for the eye. For the negative torsion rate, anti-clockwise direction (from 0° to -360°), the wavelength shift is superior compared to the wavelength shift of the clockwise direction, as presented in Fig. 3 (a) for the Bragg wavelength λ_1 of the $LP_{1,1}$ mode. However, the wavelength shifts observed for each resonance of both modes are not enough to measure the torsion response. Fig. 3 (b) shows that the normalized reflected power intensities (I_{λ_1} , I_{λ_2} , I_{λ_3} , and I_{λ_4}) from the Bragg wavelengths of each mode ($LP_{0,1}$ and $LP_{1,1}$) interchange from one to another with the applied torsion rate. This effect was already observed for a high-birefringence (Hi-Bi) fiber torsion sensor demodulated using a Hi-Bi FBG [14]. The intensity variation was compensated by a torsion parameter defined as $\eta = 10 \times \log(I_{\max}(\lambda_1)/I_{\min}(\lambda_2))$ [14]. This parameter was used to simplify the relationship between the normalized reflected power and the torsion rate and also compensate for the power intensity variations, as shown in Fig. 3 (c). The intensity response of both modes is similar and presents three linear ranges defined as slope 1, 2, and 3 at specific torsion rates. For the case of slope 1 and 2, both modes present a linear sensitivity of 0.140 ± 0.010 dB/(rad/m) in the range of -53.36 to -13.09 rad/m and 26.18 to 65.45 rad/m of the torsion rate, respectively. The slope 3 presents a linear sensitivity of -0.092 ± 0.006 dB/(rad/m) in the range of 65.45 to 117.81 rad/m. The

discrimination of the torsion direction (clockwise and anticlockwise) also is possible due to the opposite intensity response. The torsion imposed on the 4.5 μm off-axis FBG fabricated in the SMF-28e fiber caused modulation of the intrinsic birefringence. This modulation is due to the geometric rotation of the principal axes of the optical fiber and the rotation due to circular birefringence related effects (i.e., optical activity) [7], [14].

4. Conclusion

A first order off-axis FBG in an SMF-28e through fs-laser direct writing was developed. When inscribing the grating with a lateral shift of 4.5 μm from the core center, it was found that it is possible to fabricate a multimode section in the SMF-28e supporting two separate fiber modes ($\text{LP}_{0,1}$ and $\text{LP}_{1,1}$), each splits into two degenerate polarization modes. The grating structures break the cylindrical symmetry of the fiber and introduce a birefringence on the order of 10^{-4} . The birefringent off-axis FBG potential for torsion measurements was explored and a maximum linear sensitivity of 0.140 ± 0.010 dB/(rad/m) in the range of -53.36 to -13.09 rad/m and 26.18 to 65.45 rad/m of the torsion rate, respectively was achieved. Thus, the 4.5 μm off-axis FBG can simultaneously measure torsion and discriminate the direction. The relatively low complexity and the robust nature of the fabricated device open the possibility to measure the torsion and discriminate against the torsion direction in practical applications, such as structural health monitoring.

5. Acknowledgments and funding

This activity is supported by grant, SFRH/BD/110035/2015, from the Ministry of Education and Science of the Portuguese Government. The research leading to these results was developed in the framework of Project SAFE WATER - "On Chip Whispering Gallery Mode Optical Microcavities For Emerging Microcontaminant Determination In Waters", supported and co-funded by the European Commission, Directorate-General Communications Networks, Content and Technology (DG CONNECT) under the ERA-NET Cofund scheme - Horizon 2020 "Horizon 2020 – the Framework Programme for Research and Innovation (2014-2020)".

6. References

- [1] T. Erdogan, "Fiber Grating Spectra," *J. Light. Technol.*, vol. 15, no. 8, pp. 1277–1294, 1997.
- [2] R. Kashyap, *Fiber Bragg Gratings*. Academic Press, 2010.
- [3] L. Zhang, X. Qiao, Q. Liu, M. Shao, Y. Jiang, and D. Huang, "Off-axis ultraviolet-written thin-core fiber Bragg grating for directional bending measurements," *Opt. Commun.*, vol. 410, no. September 2017, pp. 197–201, 2018.
- [4] D. Feng, X. Qiao, and J. Albert, "Off-axis ultraviolet-written fiber Bragg gratings for directional bending measurements," *Opt. Lett.*, vol. 41, no. 6, p. 1201, 2016.
- [5] S. J. Mihailov, *Femtosecond Laser-Inscribed Fiber Bragg Gratings for Sensing Applications*. Elsevier Inc., 2018.
- [6] C. Koutsides, K. Kalli, D. J. Webb, and L. Zhang, "Characterizing femtosecond laser inscribed Bragg grating spectra," *Opt. Express*, vol. 19, no. 1, p. 342, 2011.
- [7] V. Budinski and D. Donagic, "Fiber-optic sensors for measurements of torsion, twist and rotation: A review," *Sensors (Switzerland)*, vol. 17, no. 3, pp. 1–29, 2017.
- [8] C. Caucheteur, T. Guo, and J. Albert, "Polarization-Assisted Fiber Bragg Grating Sensors: Tutorial and Review," *J. Light. Technol.*, vol. 35, no. 16, pp. 3311–3322, 2017.
- [9] G. Rajan, "Optical fiber sensors: Advanced Techniques & Applications," no. 1, p. 575, 2015.
- [10] D. Tentori, A. Garcia-Weidner, and C. Ayala-Díaz, "Birefringence matrix for a twisted single-mode fiber: Photoelastic and geometrical contributions," *Opt. Fiber Technol.*, vol. 18, no. 1, pp. 14–20, 2012.
- [11] D. Viveiros, J. M. Maia, V. A. Amorim, P. A. Jorge, and P. V. Marques, "Fabrication of periodic structures in optical fibers by femtosecond laser micromachining for sensing applications," in *SPIE 11207, Fourth International Conference on Applications of Optics and Photonics*, 2019, no. October, p. 69.
- [12] C. Chen, *Foundations for guided-wave optics*. John Wiley & Sons, 2006.
- [13] J. R. Grenier, L. A. Fernandes, and P. R. Herman, "Femtosecond laser inscription of asymmetric directional couplers for in-fiber optical taps and fiber cladding photonics," *Opt. Express*, vol. 23, no. 13, pp. 16760–71, 2015.
- [14] Y. L. Lo, B. R. Chue, and S. H. Xu, "Fiber torsion sensor demodulated by a high-birefringence fiber Bragg grating," *Opt. Commun.*, vol. 230, no. 4–6, pp. 287–295, 2004.